TRIUMF
Canada’s national laboratory for particle and nuclear physics
Laboratoire national canadien pour la recherche en physique nucléaire
et en physique des particules

Integral magnetic field measurement technique for a dipole magnet

Report presented to

Marco Marchetto
ISAC High Energy Facility Coordinator

By

Gaby Davilus
Co-op student

December 11, 2015

Abstract

This is a report of a project related to a coop student placement at TRIUMF. The report presents a method to measure integral magnetic field on a dipole magnet. The technique is based on Faraday’s law related to magnetic field and flux variation. The Y-30 dipole magnet was used for developing the technique. Proof of principle has been established. The aim is to improve the apparatus to reach higher sensitivity in order to map the HRS magnet.

Table of Contents

List of figures

List of tables

1. Introduction

Performing integral magnetic field measurements is one of the required steps in order to fully qualify a magnet. This report presents a technique developed to measure magnetic field integrals on a dipole magnet. The Beam Physics Group at TRIUMF is looking to an accurate method to perform these measurements for the ARIEL High Resolution Spectrometer (HRS) magnet. The magnet will be mapped by the manufacturer with an accuracy of about 1/10000, but the Group wants to reach an integral field error less than 1/100000. Since the magnet is on design and manufacturing process, another dipole magnet (Y-30 dipole magnet) has been used to develop the technique.

2. Basic specifications of the Y-30 magnet

The magnet (fig.1) is located in the Proton Hall Extension and was used for all experiments. Some important parameters for the project purpose are presented in table 1 and a typical measurement path is shown in figure 2.

Table 1: Size of the magnet [1]

Magnet length	283.2 mm
Magnet width	580 mm
Magnet height	461.2 mm
Pole length	143.2 mm
Pole width	230 mm
Clamp thickness	13 mm
Clamp width	220 mm
Air gap	53.2 mm
Max field @ I = 320A	0.740 T *

**references* [1] & [2]

Figure 1: The Y-30 dipole magnet

Comparing to the HRS magnet, dimensions and poles shape of the two dipoles magnets are completely different, but the technique we are trying to develop is generic and can apply to different dipole having different shape.

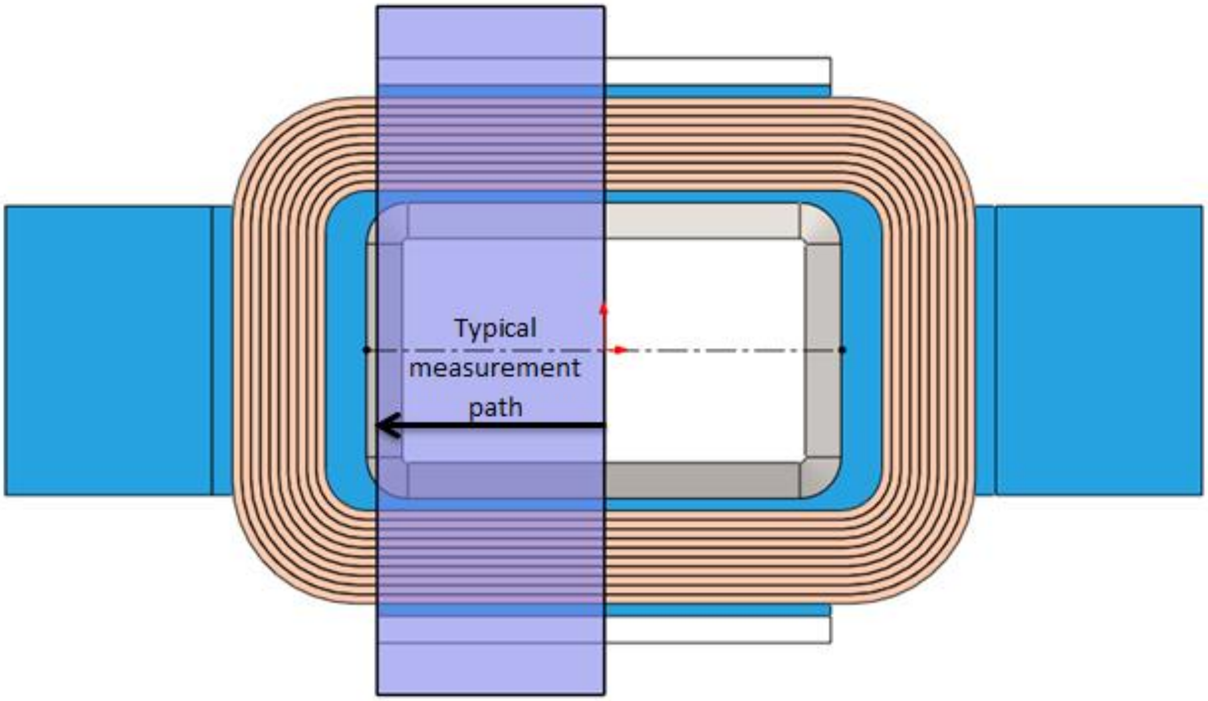

Figure 2: Pole shape and a typical measurement path of the Y-30 magnet

3. Implementation of the project

Various ideas have been pointed out; some appear to be possible and some others were a bit difficult to implement.

Kind of the idea that have been discussed:

- Using a vibrating wire
- Using rotating coils
- Moving a coil along the mid-plane…

From that point it was possible to focus on and develop one of the top ideas. Finally we have decided to try the idea of moving a coil along the mid-plane of the magnet where a change of position should generate a change of magnetic flux.

3.1. First step in the process: Test the magnet

We started with a simple test based on the principle of electromagnetic induction. The purpose of the experiment is to make sure that we can actually generate signals on the magnet. As well as to get an idea of what kind of signal we should expected in order to design appropriate coils.

In order to analyze data from the test a relation between the induce voltage (v created in the magnet) and the change in current ($d\mathrm{i}/dt$ from the power supply) is necessary.

We know that a change in current creates a change of magnetic field, and therefore flux change as well, which will then create an electric field. It is mathematically represented by the Maxwell-Faraday equation as: [3]

$$\oint_{\partial\Sigma} \mathbf{E} \cdot \mathrm{d}\boldsymbol{\ell} = -\frac{d}{dt} \iint_{\Sigma} \mathbf{B} \cdot \mathrm{d}\mathbf{S}$$

Furthermore, Faraday law states that the induced electromotive force in any closed circuit is equal to the rate of change of the magnetic flux enclosed by the circuit. [4]

This can be writing mathematically as: [5]

$$emf = -\frac{d\varphi}{dt}$$

For a coil with N identical turns of wire: [6]

$$emf = v = -N\frac{d\varphi}{dt}$$

In our case this makes reference to the sense coil of the magnet (recall small coil, N_{sc} = 30 turns) since it is the one on which induced voltage signals will be generated.

The equation that defined the magnetic flux is presented as: [3]

$$\varphi = \iint Bds$$

Since the area of the coil is constant the induce voltage can be written as:

$$v = -N_{sc}\,S\frac{dB}{dt}$$

Or the field in along the gap can be expressed as: [7]

$$B = \frac{\mu_0 N_{bc} I}{gap}$$

Where N_{bc} is the number of turns of the big coil and “gap” refers to the height of the air gap. μ_o is the magnetic permeability ($\mu_0 = 4\pi \times 10^{-7}$ $[\mathrm{H} \cdot \mathrm{m}^{-1}]$ or $[\mathrm{N}\,\mathrm{A}^{-2}]$).

We also know the linear relation between the current and the field value at the center of the Y-30 magnet, as presented in the graph at the next page (fig.3).

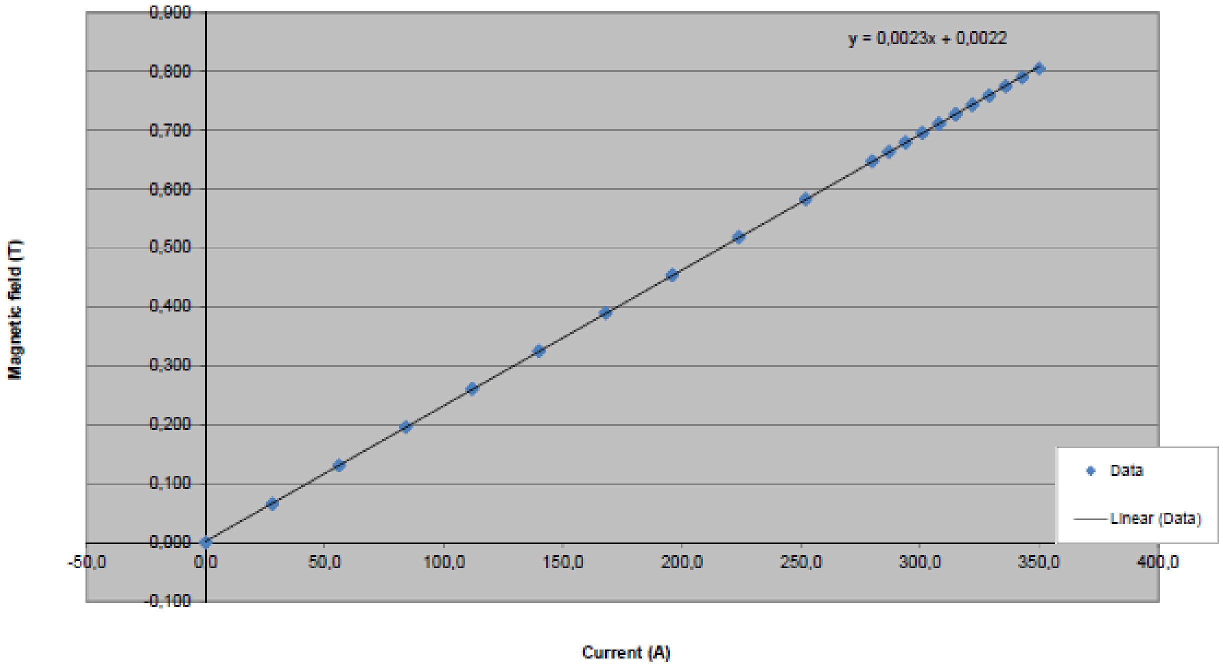

Figure 3: Relation between the current and the field value for the HRS magnet [2]

The linear trend equation of the graph states:

$$B = (2.3\, I + 2.2) \times 10^{-3}$$

This could be roughly written as in [8]:

$$B = 2.32 \times 10^{-3}\, I$$

Then the derivative of the equation gives:

$$\frac{dB}{dt} = 2.32 \times 10^{-3}\, \frac{dI}{dt}\ [T/A]$$

Finally the relation between the magnet induced voltage and the change of current is:

$$v = -\,4.9\ X\ 10^{-3}\, \frac{dI}{dt}$$

3.1.1. Experiment procedure

The magnet was set up for the experiment. The water flow tubes (inlet and outlet) were connected properly in order to control the temperature in the magnet. The power supply connection was also done properly including connection of an interlock.

The output of the small coil was connected directly to an oscilloscope in order to get voltage signal data from the magnet. Simultaneously, a DCC connected with two resistors (counts for 22 mΩ) were placed in the output cable of the power supply (input of the magnet) then connected to the same oscilloscope in order to get voltage signal data from the power supply (fig.4). Then we manually varied the current from a certain Ampere to zero and recorded data.

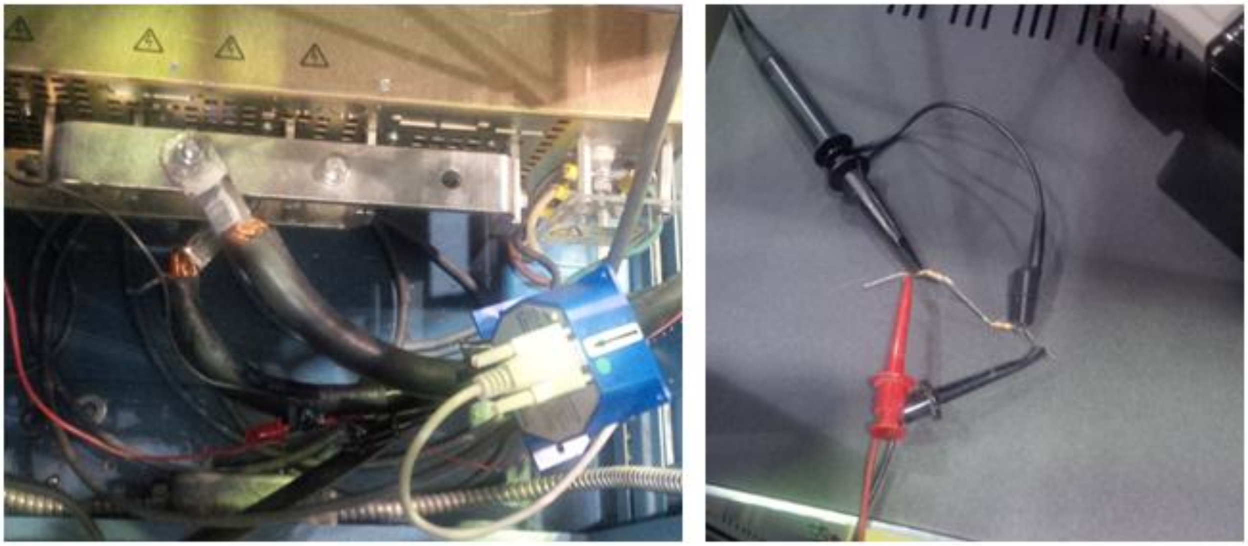

Figure 4: DCC installed to detect voltage in the cable of the power supply & resistors used

3.1.2. Result of the test

The figure below (fig.5) presents the graphs obtained for both cases, when varying the current from 30A to zero.

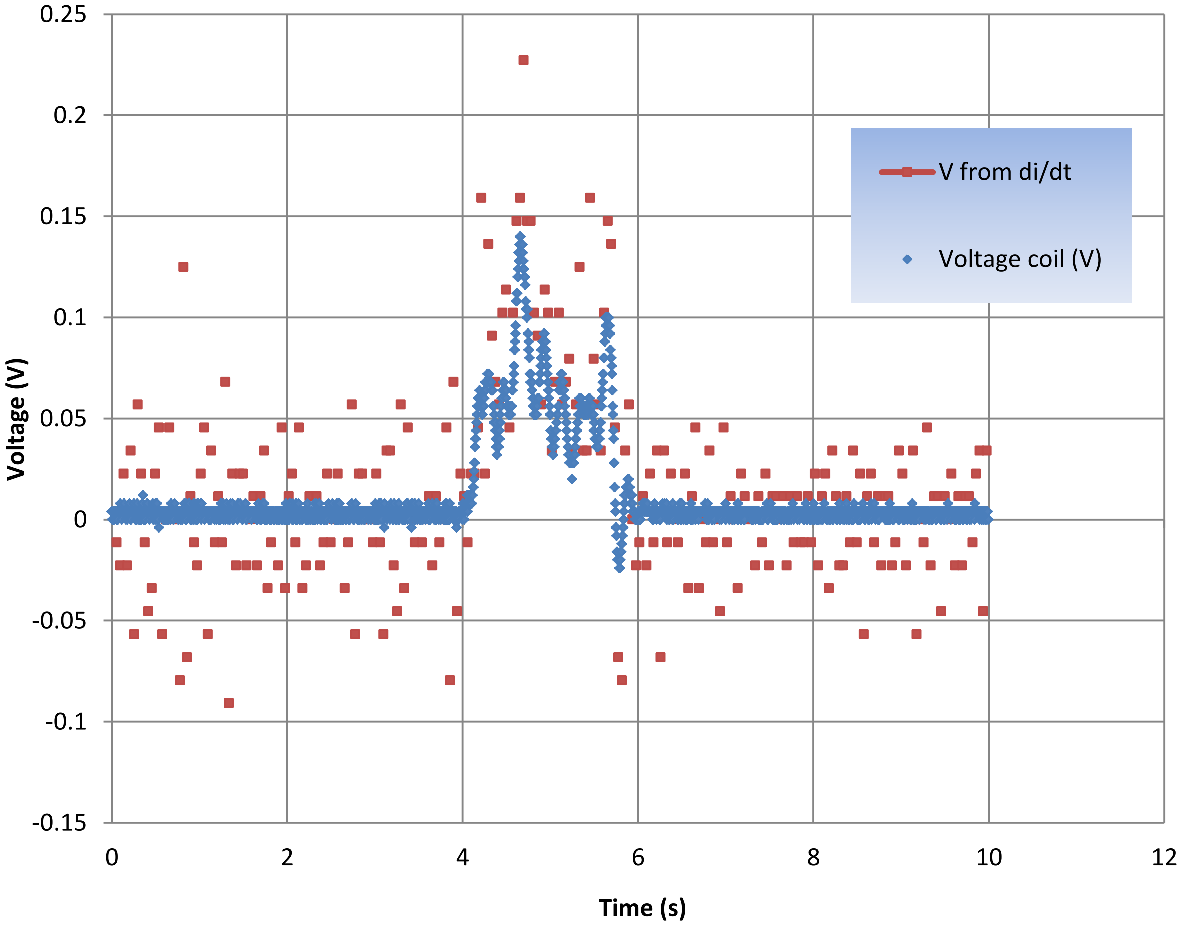

Figure 5: Comparison of the two signals obtained (magnet and power supply)

Since the results are matched we now have the certainty that the idea of using a moving coil could work.

3.2. 2nd step in the process: Start developing the technique (moving coil)

The goal is to get the integral magnetic field value for a field variation from the mid-plane of the magnet to a defined point. In other words, we want to calculate $\frac{\Delta B}{B_0}$ where B_0 is the field over the surface of the coil when it is placed directly at the center along the mid-plane and ΔB is the field difference between the two positions.

As mentioned previously, the voltage generated is given by:

$$v = -N\frac{d\varphi}{dt} = -NS\frac{dB}{dt}$$

Taking the integration of both sides and knowing that the area of the coil is constant:

$$\int vdt = -NS\int dB$$

In our case the flux is directly used without considering the field that is not constant over the surface of the coil. However, a simplification of the difference in magnetic field can be written as:

$$\Delta B = -\frac{\int vdt}{NS} \quad or \quad \Delta B = -\frac{\Delta\varphi}{NS}$$

Since it's not possible to get any absolute magnitude values of the field with this technique, in order to calculate $\frac{\Delta B}{B_0}$, the value of B_0 obtained in the magnet model (from OPERA) will be used.

3.2.1. Experiment procedure

Like the previous experiment the magnet was set up with the same water flow, same power supply and interlock. Furthermore, the same oscilloscope was used to record data.

To start, a jig that had been used to make experiments with a Hall probe in the same magnet has been used to make a coil of 50 turns (fig.6). We take the advantage that the jig was machined to fit the gap and also it has a hole that coincides with the mid-plane of the magnet, on which we can easily make a loop. Then we connected the coil to the oscilloscope and moved it along the mid-plane of the magnet.

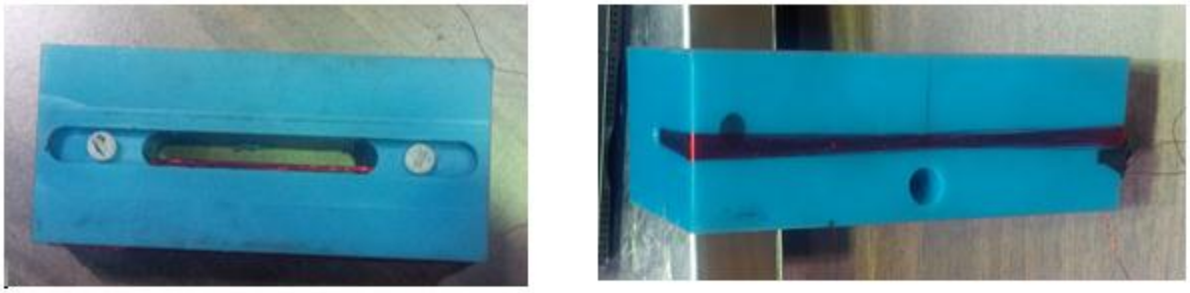

Figure 6: Blue jig with a coil of 50 turns, dimension 150mm X 30mm

3.2.2. Results of the test

The magnet was powered to 100 A. The coil is moved along the mid-plane from the center to approximately 110 mm to the left. The following signal was obtained (fig.7).

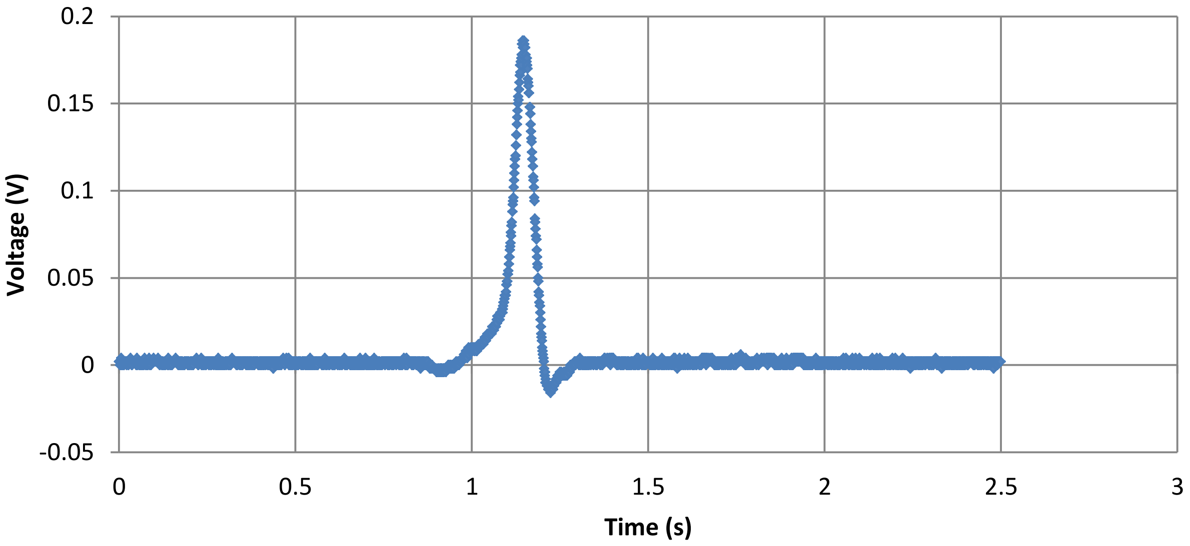

Figure 7: Signal obtained when moving the coil (blue) from the center to 110mm

The integration of the above graph gives:

$$\int vdt = 0.015958\, Tm^2$$

Then the difference in magnetic field is found to be:

$$\Delta B = 7.0\ \times 10^{-2}\mathrm{T}$$

3.2.3. Verification of the results with Opera

The Y-30 magnet model in Opera is used to verify the results of the experiment.

Information from the test:

- Coil parameters: 50 turns for an area of 150mm X 30mm
- Displacement along the mid-plane: from center to 110mm to the left
- Operating current: 100A

Output results from Opera for an operating current of 320A:

- Flux at the center : 3083.715 Tmm^2
- Flux at 110 mm : 2300.369 Tmm^2

Therefore the magnetic fields are: B_0 = 0.68527 T and B_{110} = 0.51119 T

When scaled to 100A: B_0 = 0.21415 T and B_{110} = 0.15975 T

The difference gives: $\Delta B = 5.4 \times 10^{-2}$T

Table 2: Comparison of the experimental values with the model in Opera

	Value from the experiment	Value from the model
$\Delta B\ (T)$	$7.0\ \times 10^{-2}$	5.4×10^{-2}
$\Delta B/B_0$	$3.3\ \times 10^{-1}$	$2.5\ \times 10^{-1}$

As we can see in table 3, the values have the same order of magnitude and roughly similar. Coming on that point, it was clear that we can continue to work on the technique by looking for improving it to get better results.

3.3. 3rd step: Design a jig to move coils along the mid-plane

The goal is to get a mechanism that will allow precise displacements when moving coils along the mid-plane.

3.3.1. A first idea

At the beginning we were thinking about a structure that can be locked directly inside the gap of the magnet, on which a coil could be freely moved. For instance we were trying to build a structure as presented in the figure below (fig.8). The mechanisms placed on each end should ensure the fixation of the structure in the magnet gap. The mechanism that supports the coil (the square mechanism) is free to move along the two rods. Two stoppers are added in order to move the coil along a defined distance. The coil support should be able to fit any dimension of coils, as soon as they can fit the gap of the magnet. An example of a cylindrical coil is actually mounted on the support.

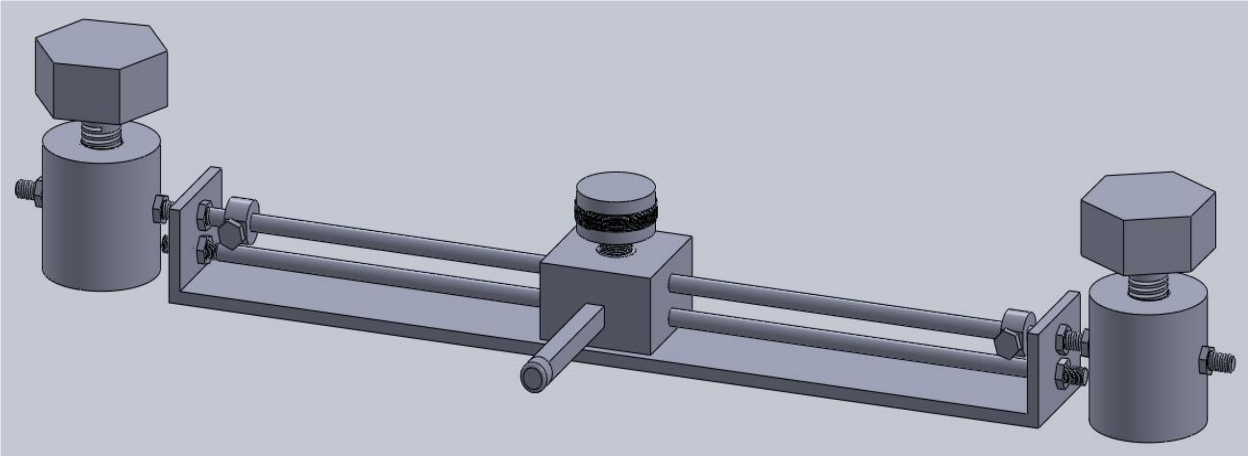

Figure 8: First attempt on developing a structure to move coils along the mid-plane

The idea seems interesting but there would be some difficulty to install this structure exactly in the mid-plane as the gap is a bit small. Furthermore, it is not guaranteed that the rods won't shake; what we need to avoid. Therefore we are looking to have an alternative solution.

3.3.2. An idea that works

After taking advices, particularly from a senior mechanical machinist, we have decided to develop the structure presented in the figures below (fig.9). It can supports whether a small or a long coils. It can simply calibrate on the magnet clamps. The motion path is precisely defined by using two stoppers that would be fixed in the clamp as presented in the figure.

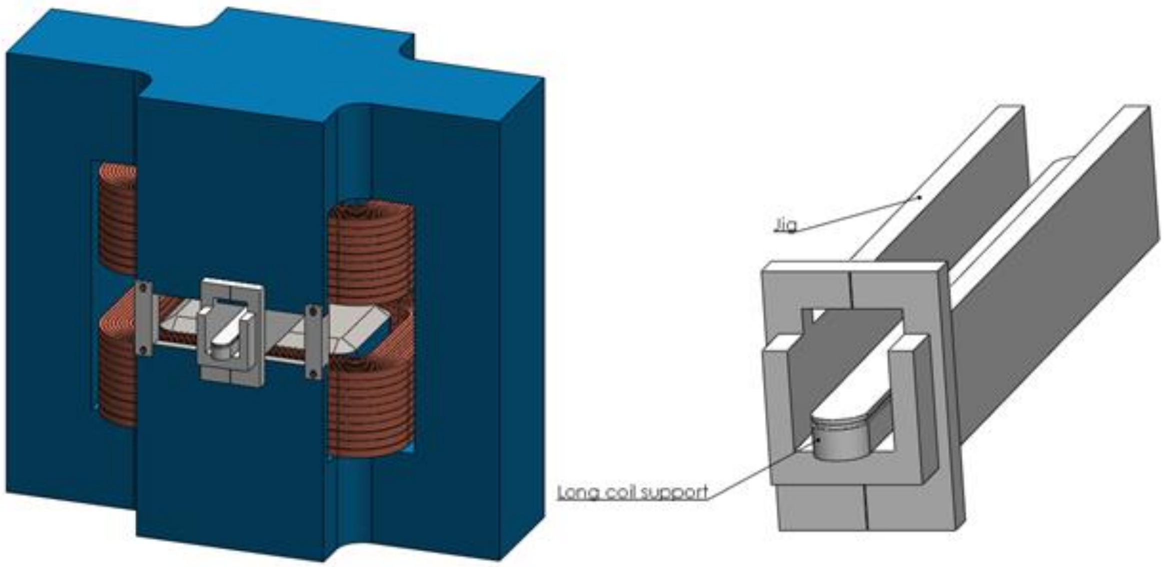

Figure 9: Sketch of the jig used to move the coils

Two different shapes of coil support have been designed for the experiments (fig.10).

- A long coil support (389.6 mm X 20 mm)
- 3 small cylindrical coil supports (5 mm, 10 mm and 20 mm diameters)

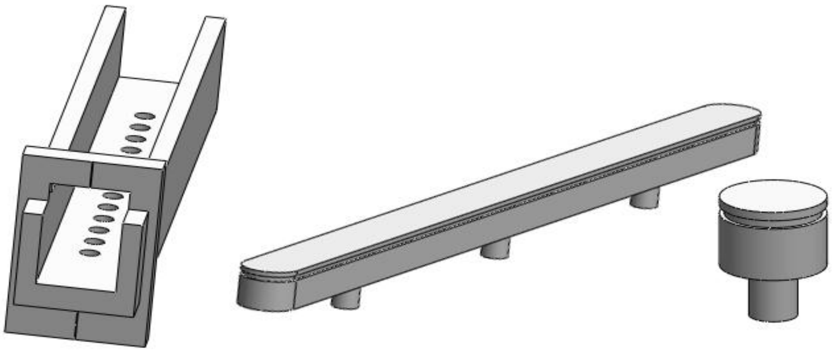

Figure 10: The jig and two of the coil supports

All parts were machined here at TRIUMF with precise dimensions (see appendix 2 for more details). The final products are presented in figures below (fig.11 and fig.12), all parts are in nylon, delrin in particular, and the stoppers' crews are in aluminum.

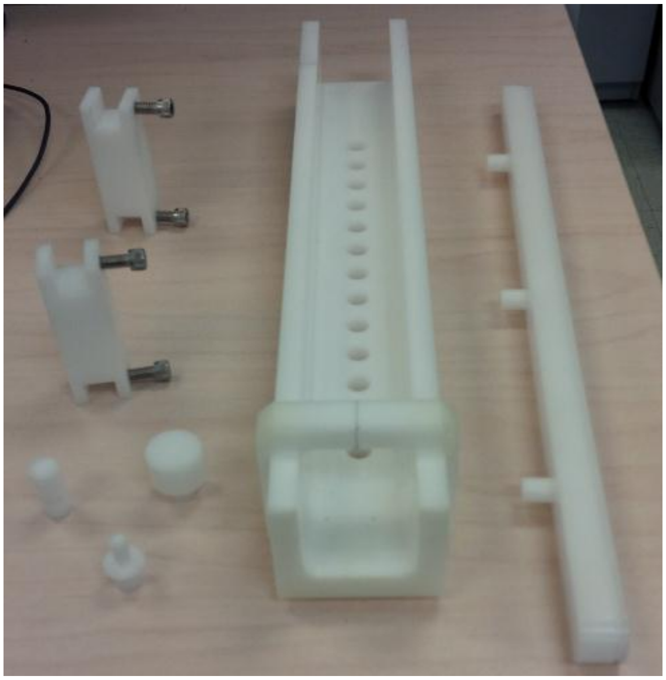

Figure 11: Jig, coil supports and stoppers

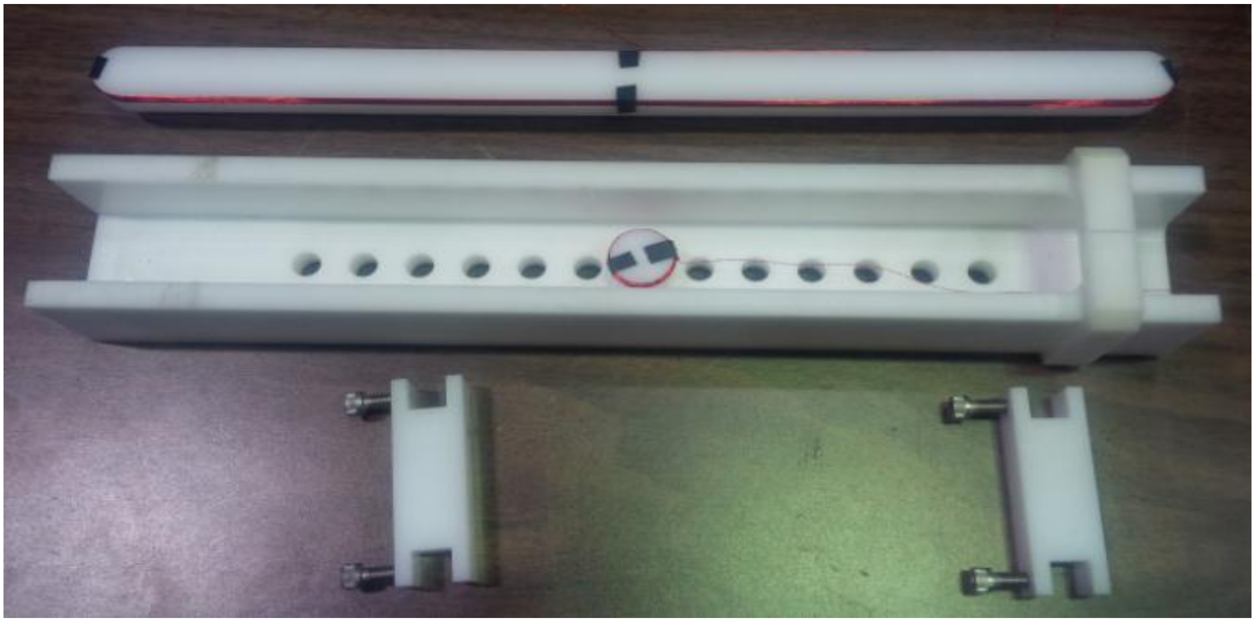

Figure 12: Jig, supports with actual coils and stoppers

3.3.3. Experiment procedure

Two coil supports were selected to start with, the long one and the small cylindrical of 20 mm diameter. A loop of 100 turns of wire was done around both supports as shown in the previous figure (fig.12). The previous coil (the blue jig with 50 turns) will be used again for verification as we will use a new system to record data in addition to the oscilloscope.

The magnet was set up with the same water flow; same power supply and interlock as the previous experiments. The power supply was set up at 250A to increase the signal. And later the results from the model were scaled in order to compare the values.

In addition to the oscilloscope a digital multi-meter (DMM) was used. The multi-meter was connected directly to a computer running Epics software. The software was programmed to generate the induce voltage signals (similar to the oscilloscope) but also the integration value of the signal with respect to time. In other words it was possible to obtain the magnetic flux difference between two selected positions directly from Epics.

Note that the stoppers weren’t really used when performing the tests because we have recorded some disturbances in the signals each time the jig reached a stopper. Alternatively desired positions were carefully marked using a pencil (fig.13).

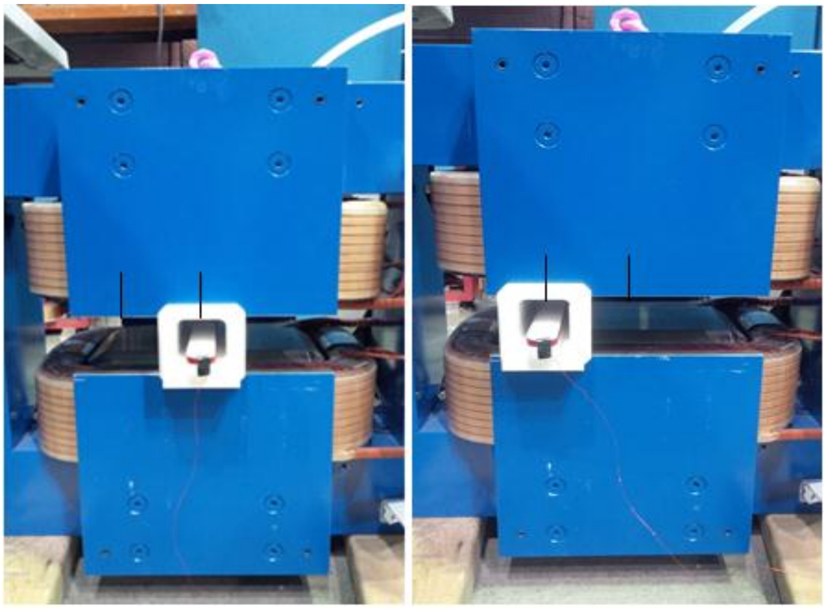

Figure 13: Long coil moved from the center to 65 mm to the left

3.3.4. Results

Using the 3 coils mentioned above several tests was performed for different defined displacement starting from the centre of the magnet. Two samples are presented here. See appendix 1 for more samples.

3.3.4.1. Signal obtained when moving the long coil from center to 65mm (Figures 14, 15 & 16)

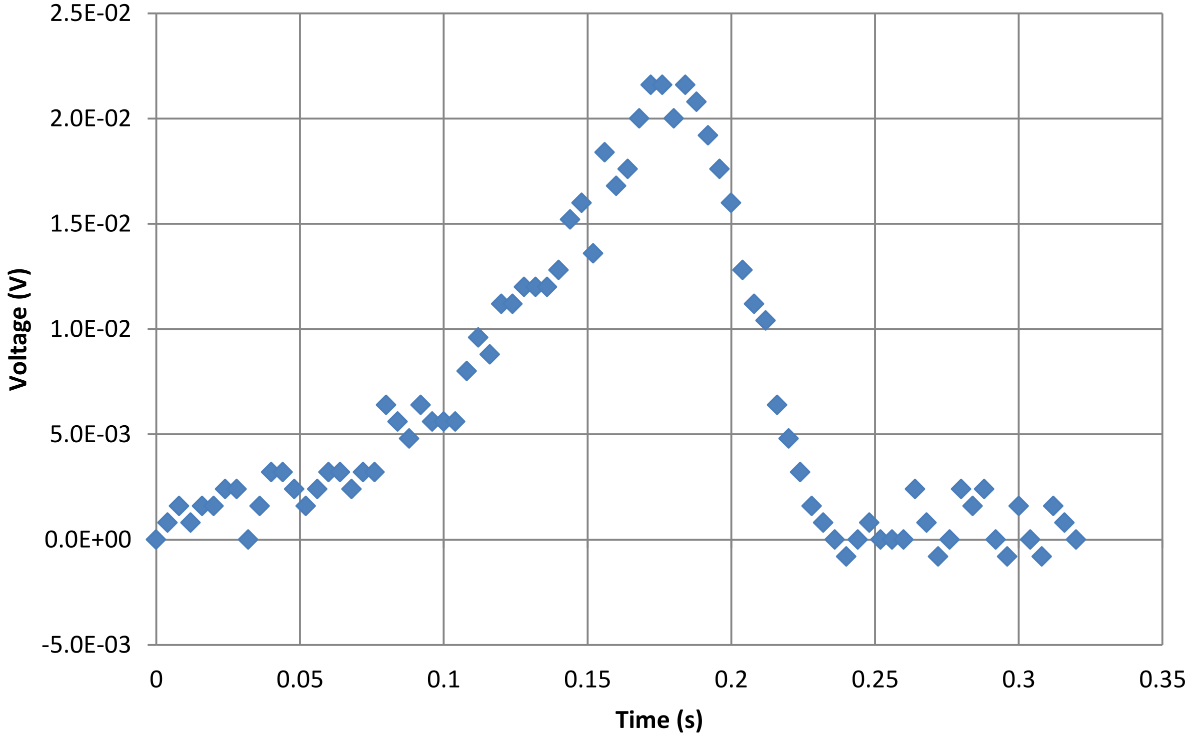

Figure 14: Voltage data obtained with the oscilloscope

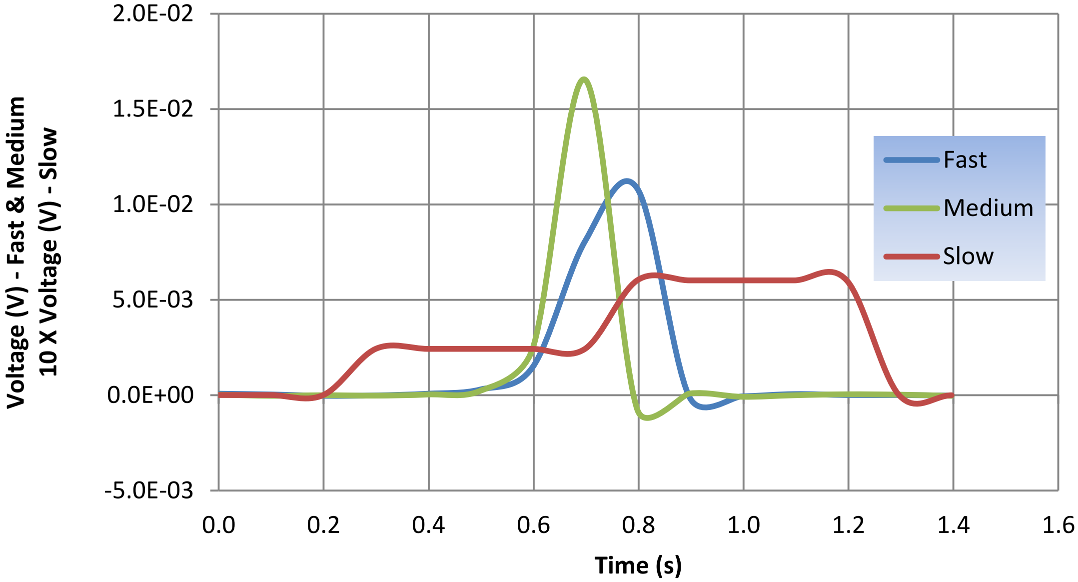

Figure 15: Voltage data from Epics with 3 different DMM update rate

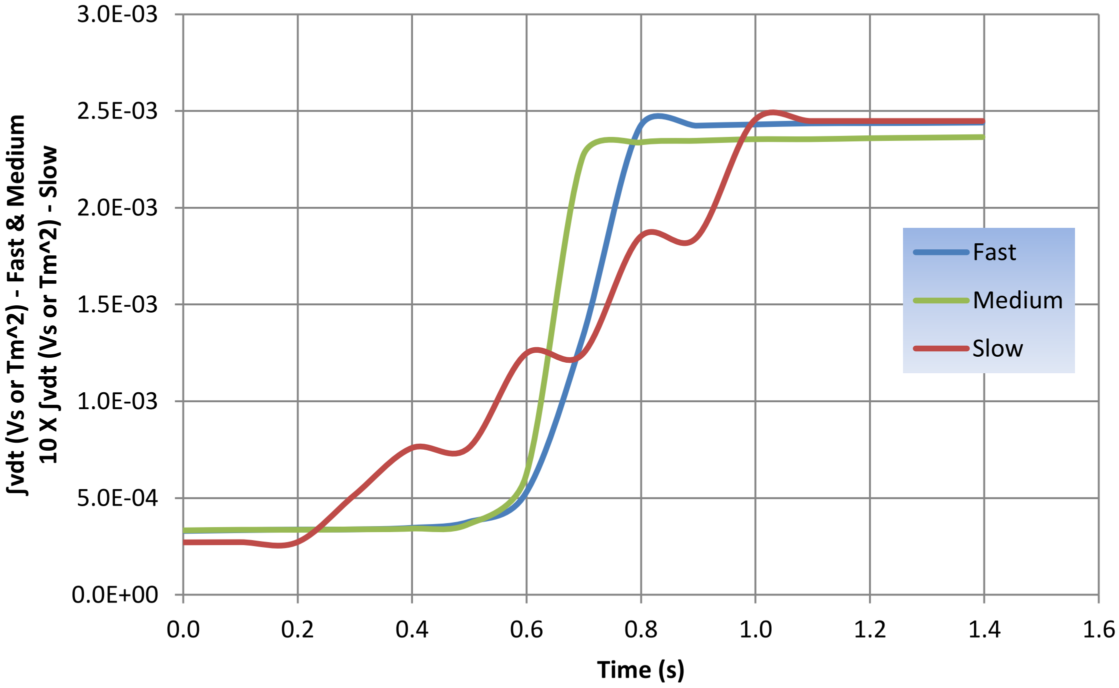

Figure 16: Integration data from Epics with 3 different DMM update rates

3.3.4.2. Signal obtained when moving the small cylindrical coil from center to 95mm (Figures 17, 18 & 19)

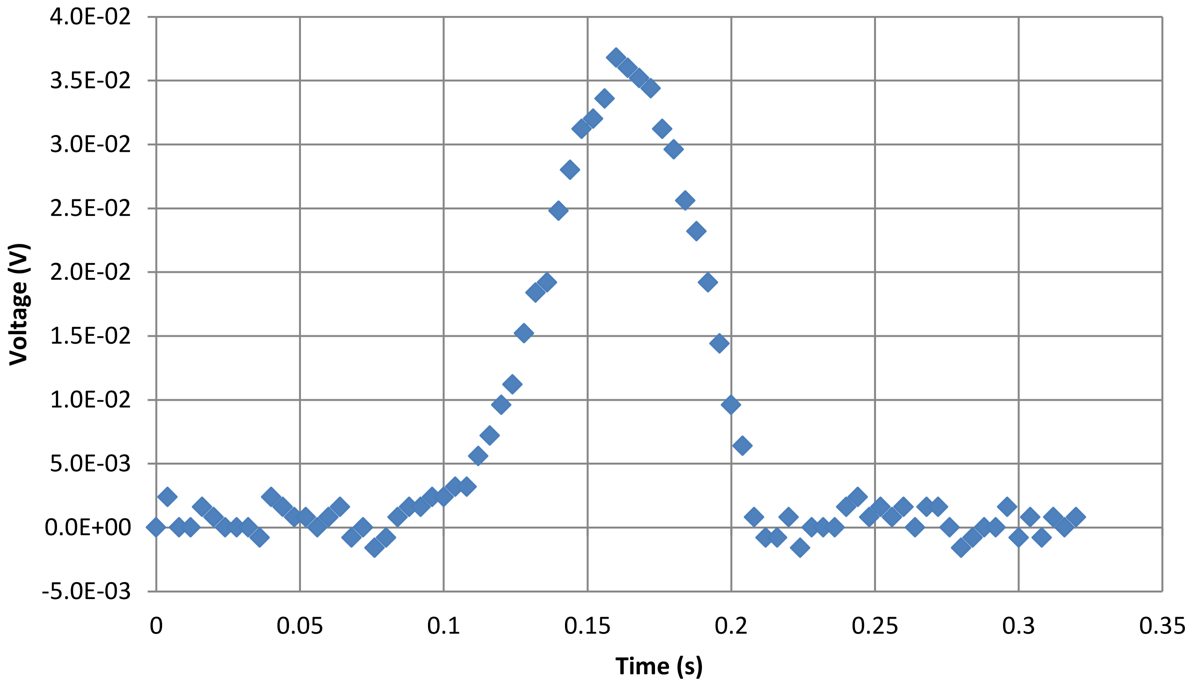

Figure 17: Voltage data obtained with the oscilloscope

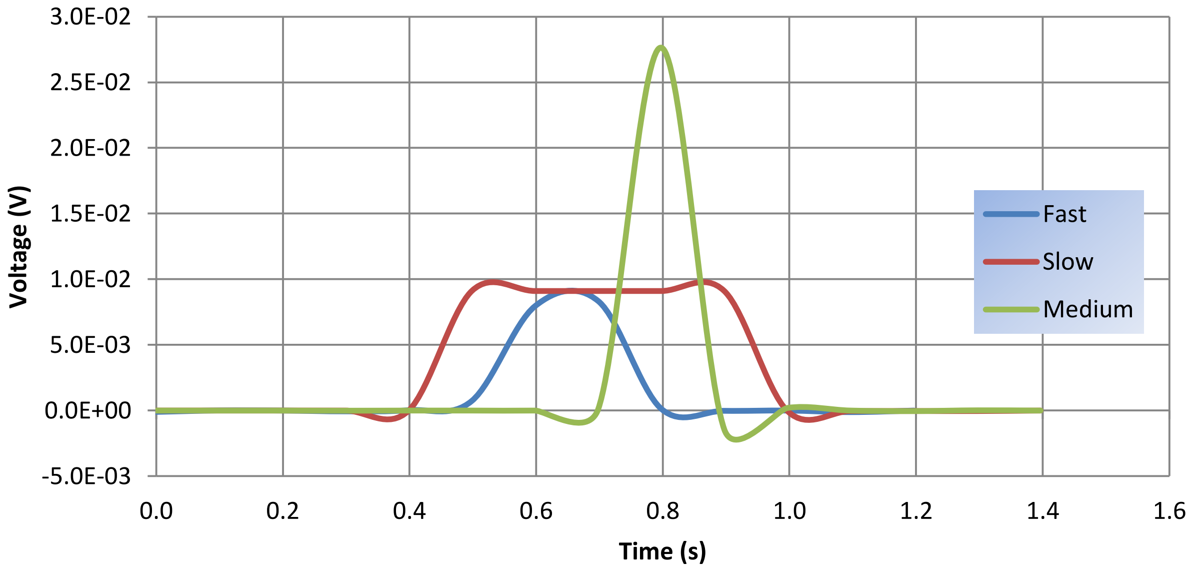

Figure 18: Voltage data from Epics with 3 different DMM update rate

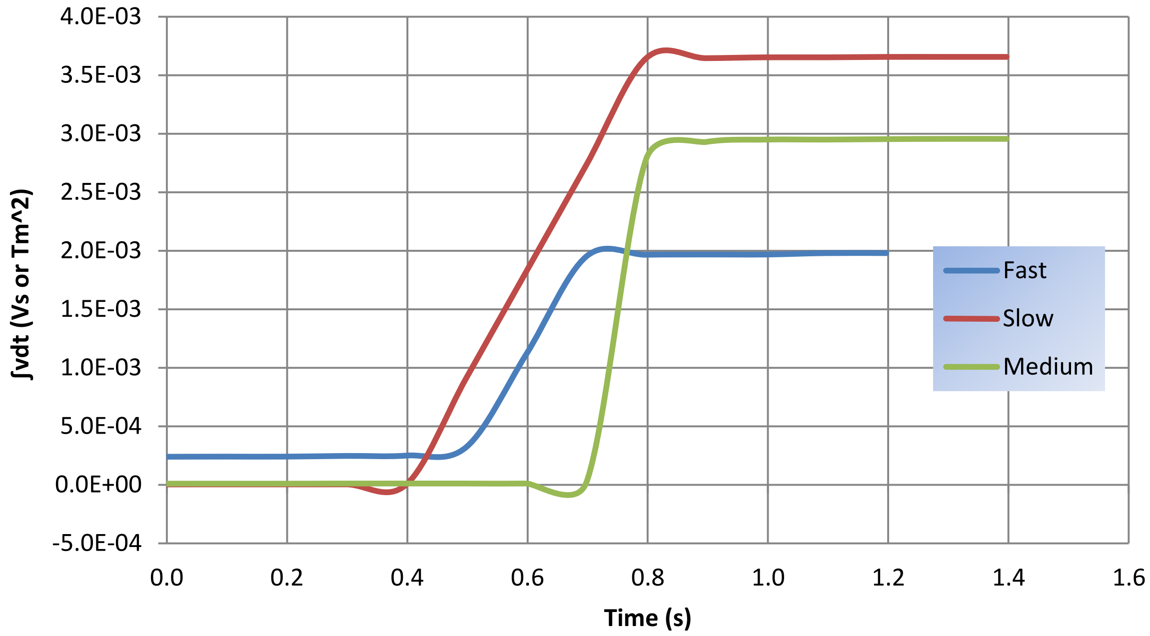

Figure 19: Integration data from Epics with 3 different DMM update rates

3.3.5. Verification of the results with Opera

Output results from Opera for the long coil with an operating current of 320A:

- Flux at the center : 2557.5253 Tmm^2
- Flux at 65 mm : 2535.9002 Tmm^2

Output results from Opera for the small cylindrical with an operating current of 320A:

- Flux at the center : 232.8974 Tmm^2
- Flux at 95 mm : 212.3265 Tmm^2

All these values are then scaled to 250A in order to make the comparison.

Table 3: Comparison table of results obtained when moving the long coil from center to 65mm

	Expectations (model)		
φ @ center (Tm^2)	2.00E-03		
φ @ 65mm (Tm^2)	1.98E-03		
ΔB/Bo	**8.46E-03**		
	Scope	**Epics Integration from Excel**	**Direct integration from Epics**
Fast*			
∫vdt or Δφ (Tm^2)	2.25E-03	2.06E-03	2.11E-03
∫vdt/N (Tm^2)	2.25E-05	2.06E-05	2.11E-05
ΔB/Bo	**1.13E-02**	**1.03E-02**	**1.06E-02**
Medium*			
∫vdt or Δφ @ (Tm^2)	2.07E-03	1.85E-03	2.04E-03
∫vdt/N (Tm^2)	2.07E-05	1.85E-05	2.04E-05
ΔB/Bo	**1.03E-02**	**9.26E-03**	**1.02E-02**
Slow*			
∫vdt or Δφ (Tm^2)	2.05E-03	4.22E-04	2.18E-04
∫vdt/N (Tm^2)	2.05E-05	4.22E-06	2.18E-06
ΔB/Bo	**1.03E-02**	**2.11E-03**	**1.09E-03**

*DMM Update rate

Table 4: Comparison table of results obtained when moving the small cylindrical coil from center to 95mm

	Expectations (model)		
φ @ center (Tm^2)	1.82E-04		
φ @ 95mm (Tm^2)	1.66E-04		
ΔB/Bo	**8.83E-02**		
	Scope	**Epics Integration from Excel**	**Direct integration from Epics**
Fast*			
$\int vdt$ or Δφ (Tm^2)	2.23E-03	1.69E-03	1.74E-03
$\int vdt/N$ (Tm^2)	2.23E-05	1.69E-05	1.74E-05
ΔB/Bo	**1.23E-01**	**9.29E-02**	**9.56E-02**
Medium*			
$\int vdt$ or Δφ (Tm^2)	2.29E-03	2.64E-03	2.95E-03
$\int vdt/N$ (Tm^2)	2.29E-05	2.64E-05	2.95E-05
ΔB/Bo	**1.26E-01**	**1.45E-01**	**1.62E-01**
Slow*			
$\int vdt$ or Δφ (Tm^2)	2.34E-03	4.53E-03	3.65E-03
$\int vdt/N$ (Tm^2)	2.34E-05	4.53E-05	3.65E-05
ΔB/Bo	**1.29E-01**	**2.49E-01**	**2.01E-01**

*DMM Update rate

4. Conclusion and future work

The results satisfy the expectation values for the selected intervals. An integral field value with a factor of 10^{-3} could be reached, particularly with the long coil. We will continue to work on the measurement technique in order to improve the results since the goal is to reach at least a factor of 10^{-5}. In fact, improvement could be possible by increasing the number of wire turns for the long coil. The obtained results are promising; the technique can most likely be applied to the HRS dipole magnet.

References

[1] T. Planche, "ARIEL 'Y30' dipole design note," TRIUMF, Vancouver, July 25, 2013.

[2] U. H. Johansen, "Magnetic Test and Quality Assurance Report for the Y-30 Dipole Magnet," DANFYSIK, Taastrup, March, 2014.

[3] R. F. Harrington, Introduction to Electromagnetic Engineering, Mineola: Dover Publications, 2003.

[4] W. Hayt, Engineering Electromagnetics, McGraw-Hill, 1989.

[5] J. Edward and B. K. G., Electromagnetic Waves and Radiating Systems, Prentice-Hall, 1968.

[6] C. R. Nave, "HyperPhysics "Faraday's Law"," Georgia State University, 29 August 2011. [Online]. Available: http://hyperphysics.phy-astr.gsu.edu/hbase/electric/farlaw.html. [Accessed 7 December 2015].

[7] B. A. S. Ruth W. Chabay, Electrical and Magnetic Interactions, Wiley, 2015.

[8] T. Planche, "Beam Physics Group Internal Server - TRIUMF," [Online]. Available: http://beamphys.triumf.ca/bp/. [Accessed 5 October 2015].

Appendix 1: Experiment results

Signal obtained when moving the long coil from center to 72 mm (figures 20, 21 & 22)

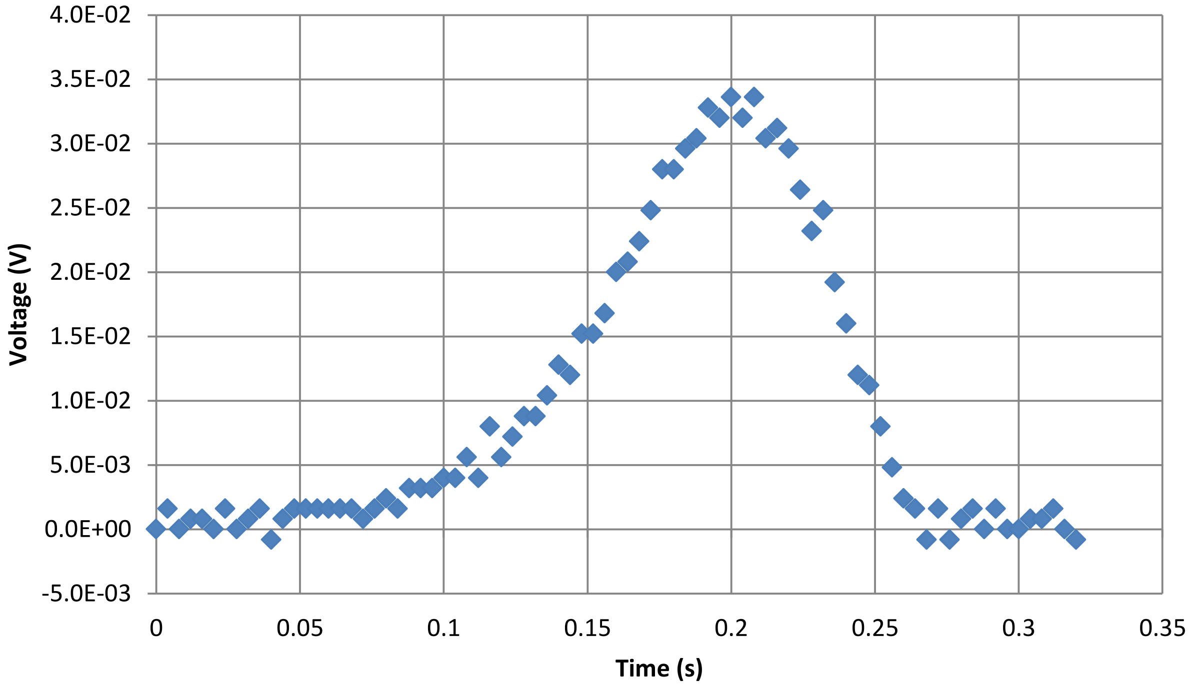

Figure 20: Voltage data obtained with the oscilloscope

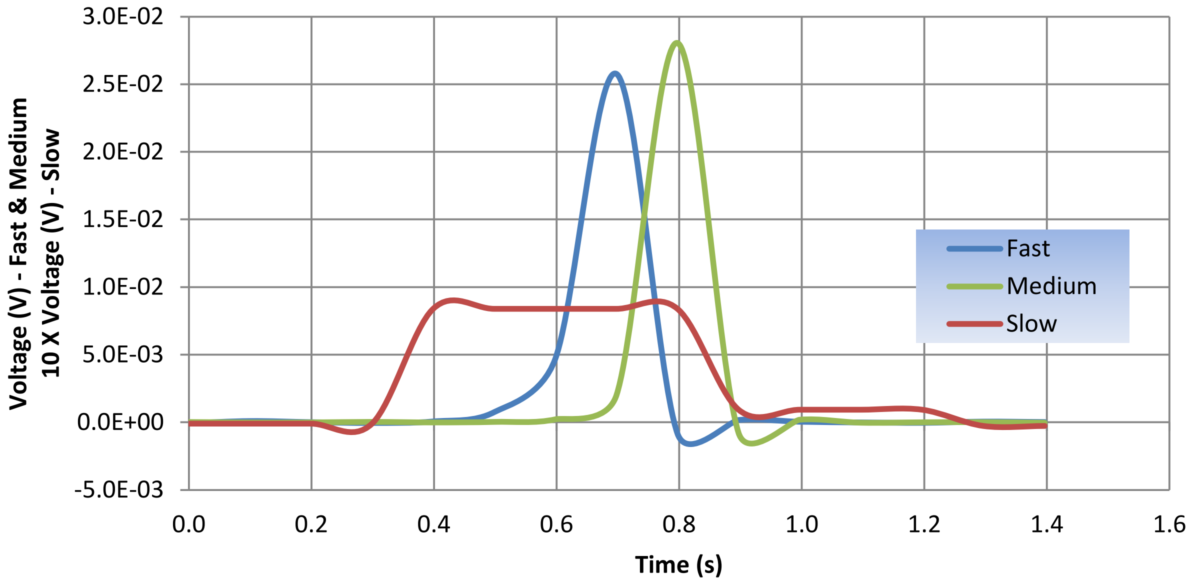

Figure 21: Voltage data from Epics with 3 different DMM update rate

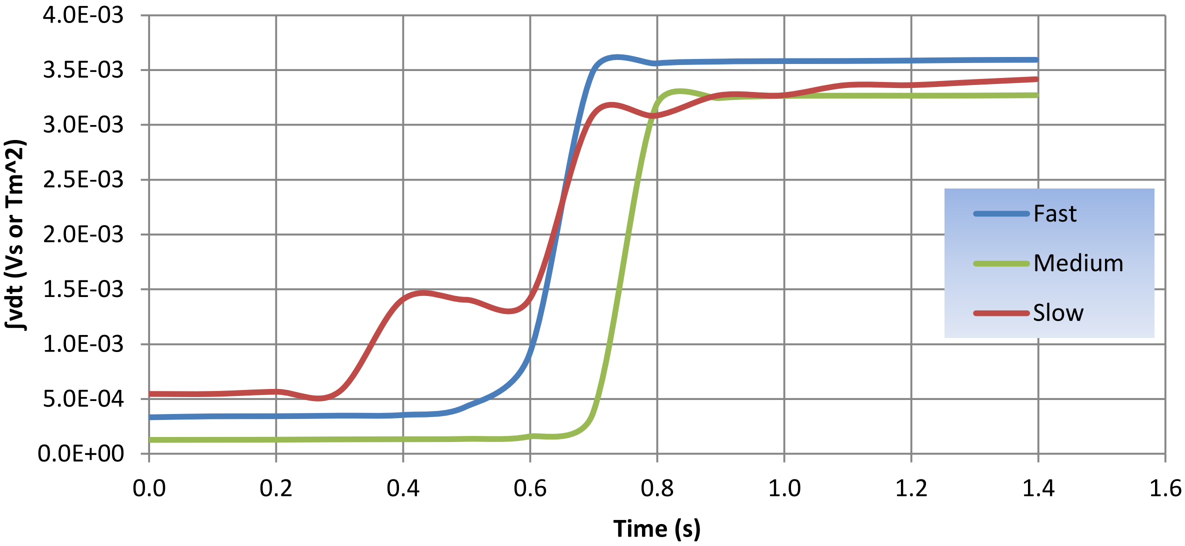

Figure 22: Integration data from Epics with 3 different DMM update rates

Signal obtained when moving the long coil from center to 78 mm (figures 23, 24 & 25)

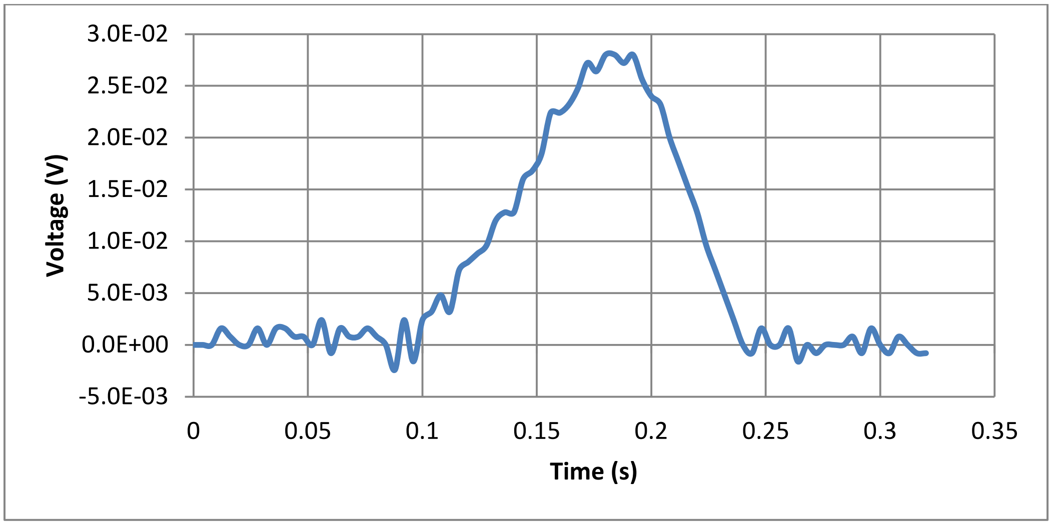

Figure 23: Voltage data obtained with the oscilloscope

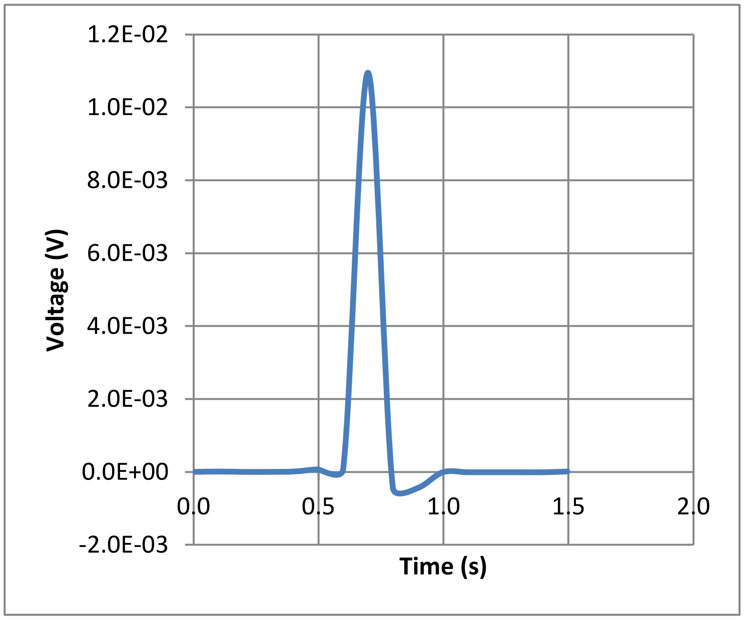

Figure 24: Voltage data from Epics

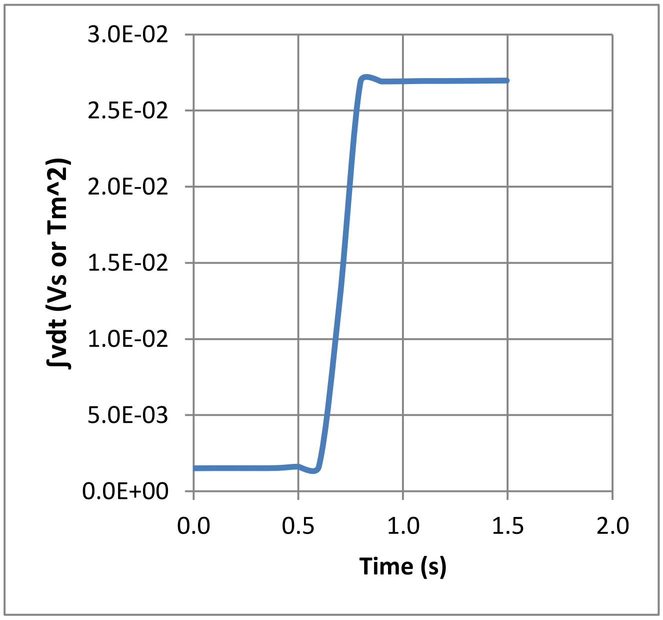

Figure 25: Integration data from Epics

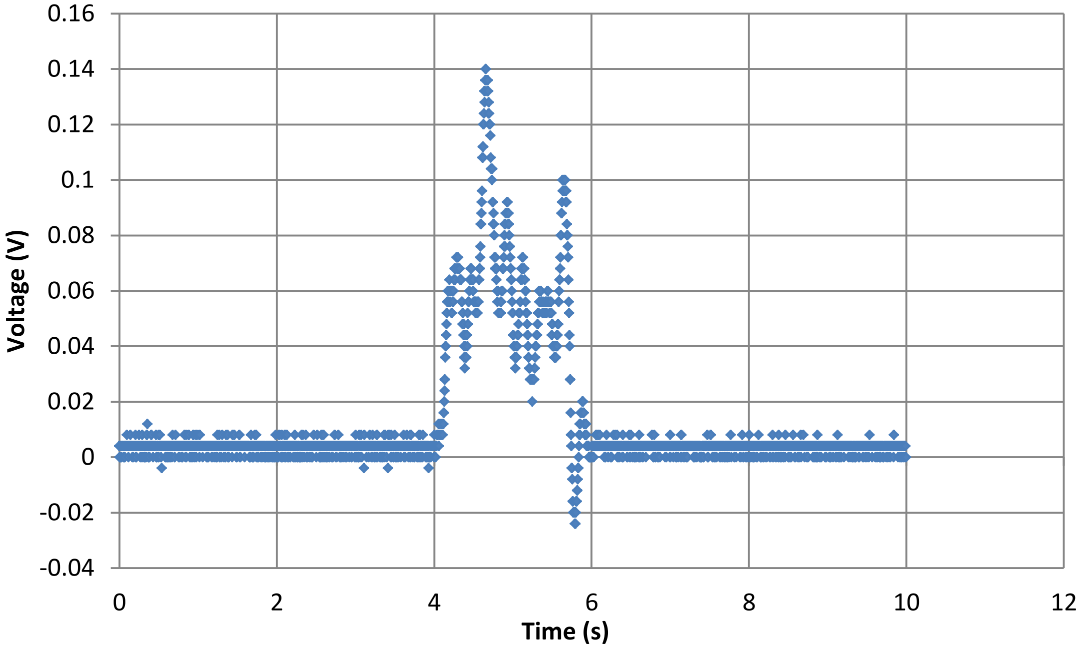

Figure 26: Voltage data from the magnet when varying the current from 30A to zero

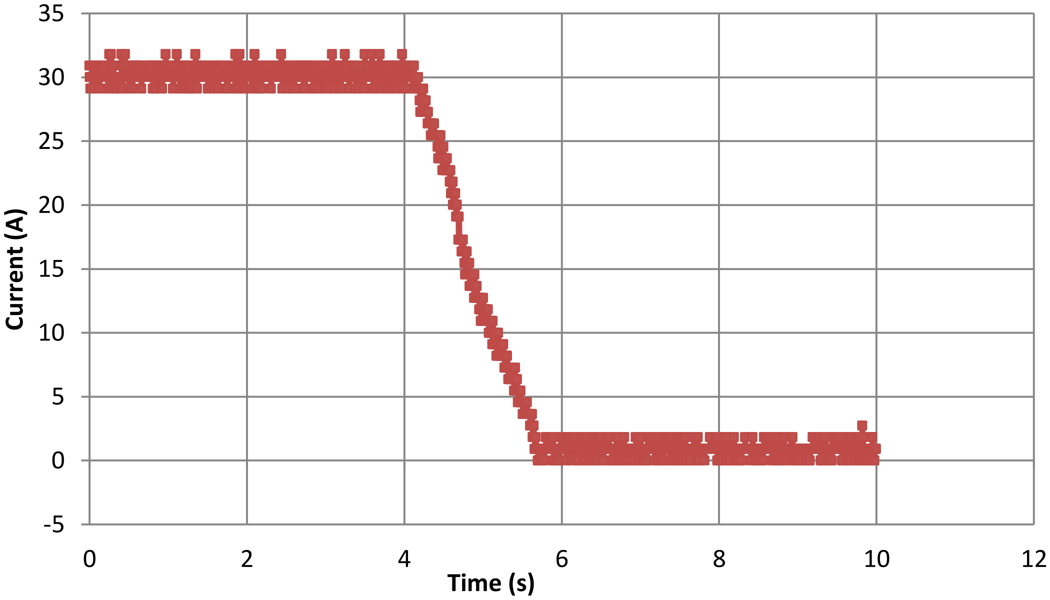

Figure 27: Variation of current in the power supply (from 30A to 0)

Table 5: Comparison table of results obtained when moving the long coil from center to 72mm

	Expectations (model)
ϕ @ center (Tm^2)	2.00E-03
ϕ @ 72mm (Tm^2)	1.97E-03
ΔB/Bo	1.53E-02

	Scope	**Epics Integration from Excel**	**Direct integration from Epics**
Fast*			
∫vdt or Δϕ @ 0-72mm (Tm^2)	3.48E-03	3.06E-03	3.26E-03
∫vdt/N (Tm^2)	3.48E-05	3.06E-05	3.26E-05
ΔB/Bo	1.74E-02	1.53E-02	1.63E-02
Medium*			
∫vdt or Δϕ @ 0-72mm (Tm^2)	3.15E-03	2.95E-03	3.14E-03
∫vdt/N (Tm^2)	3.15E-05	2.95E-05	3.14E-05
ΔB/Bo	1.58E-02	1.48E-02	1.57E-02
Slow*			
∫vdt or Δϕ @ 0-72mm (Tm^2)	3.65E-03	4.48E-04	2.87E-04
∫vdt/N (Tm^2)	3.65E-05	4.48E-06	2.87E-06
ΔB/Bo	1.83E-02	2.24E-03	1.44E-03

*DMM Update rate

Table 6: Comparison table of results obtained when moving the long coil from center to 78mm

	Expectations (model)
ϕ @ center (Tm^2)	2.00E-03
ϕ @ 78mm (Tm^2)	1.95E-03
ΔB/Bo	2.56E-02

	Scope	**Epics Integration from Excel**	**Direct integration from Epics**
Fast*			
∫vdt or Δϕ @ 0-78mm (Tm^2)	6.26E-03	6.87E-03	5.86E-03
∫vdt/N (Tm^2)	6.26E-05	6.87E-05	5.86E-05
ΔB/Bo	3.14E-02	3.44E-02	2.93E-02
Medium*			
∫vdt or Δϕ @ 0-78mm (Tm^2)	2.28E-03	1.01E-03	2.55E-03
∫vdt/N (Tm^2)	2.28E-05	1.01E-05	2.55E-05
ΔB/Bo	1.14E-02	5.08E-03	1.27E-02
Slow*			
∫vdt or Δϕ @ 0-78mm (Tm^2)	5.86E-03	2.86E-03	1.74E-03
∫vdt/N (Tm^2)	5.86E-05	2.86E-05	1.74E-05
ΔB/Bo	2.93E-02	1.43E-02	8.71E-03

*DMM Update rate

Appendix 2: Drawings

All dimensions are in millimeter.

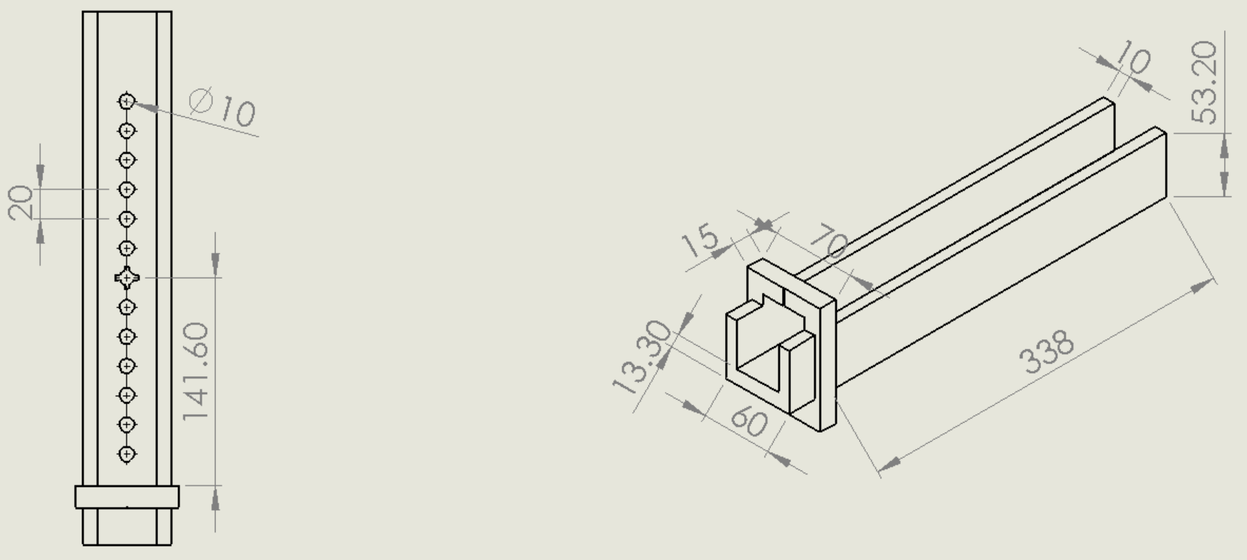

Figure 28: Drawing of the jig

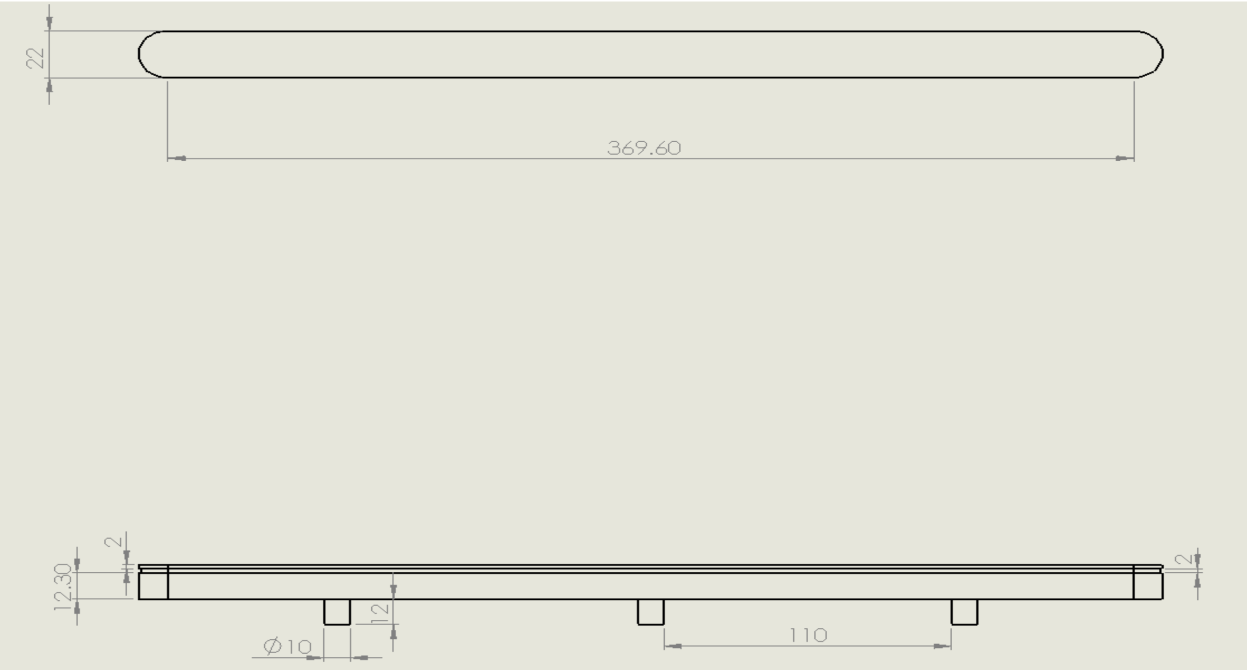

Figure 29: Drawing of the long coil support

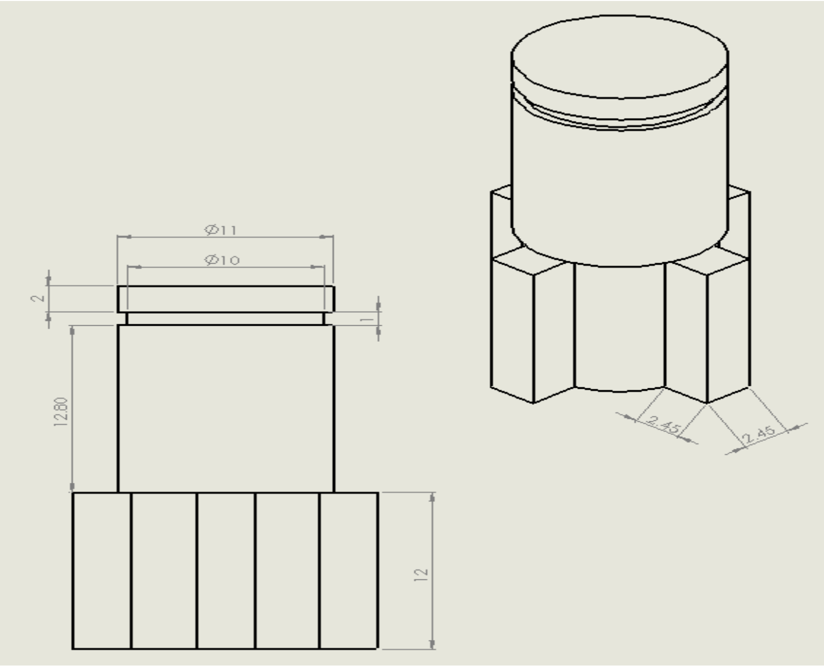

Figure 30: Drawing of the small cylindrical coil support (10 mm diam)

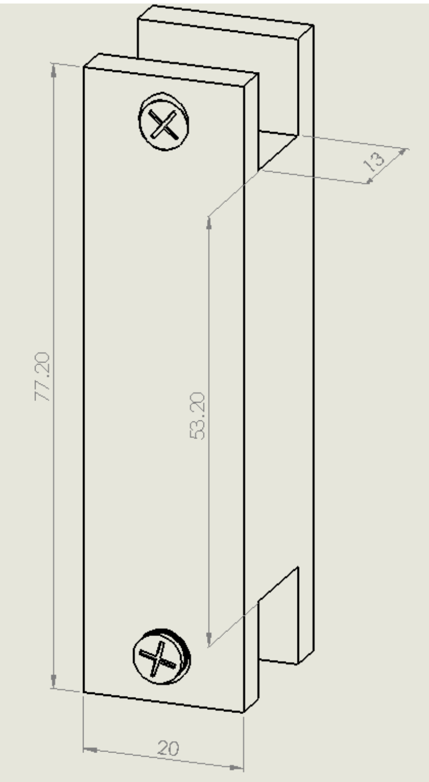

Figure 31: Drawing of the stoppers